Updates of PDFs for the 2nd LHC run

Patrick Motylinski[a,1], Lucian Harland-Lang[a], Alan D. Martin[b], Robert S. Thorne[a]

[a]*Department of Physics and Astronomy, University College London, WC1E 6BT, UK*
[b]*Institute for Particle Physics Phenomenology, Durham University, DH1 3LE, UK*

Abstract

I present results on continuing updates in PDFs within the framework now called MMHT14 due to both theory improvements and the inclusion of new data sets, including most of the up-to-date LHC data. A new set of PDFs is essentially finalised, with no changes expected to the PDFs presented here.

It has been more than five years since the publication of the global PDF analysis by MSTW titled 'Parton distributions for the LHC' [1]. Since then there have been several significant improvements in the data, in particular from the measurements made at the LHC, and it appears to be time for an new global PDF analysis within the previous MSTW08 (but now called MMHT14) framework.

As new data have become available they have been compared to the predictions provided by the MSTW PDFs. In the process we continued to use the extended parametrisation with Chebyshev polynomials as well as the freedom in deuteron nuclear corrections [2]. This leads to a change in the $u_V - d_V$–distribution. Furthermore, we use the optimal GM-VFNS choice [3] with its increased smoothing near the heavy flavour transition point. A small correction to the dimuon production ($\nu + N \rightarrow \mu^+\mu^-$) has been taken into account for the case where the charm quark is produced away from the interaction point [4]. This has an impact, albeit rather small, on the strange distribution. Furthermore, issues regarding the charm branching fraction have been addressed. The value has been changed to $B_\mu = 0.092 \pm 10\%$ from [5] where the uncertainty is being fed into the PDFs. In the MMHT framework we use the multiplicative definition of correlated uncertainties instead of additive [6]. This way the uncorrelated errors effectively scale with the data.

1. Changes in data sets

We include new data that were officially published at the end of 2013.

There has been several additions of non-LHC sets, which should be mentioned here. The HERA run I neutral- and charged current data from both HERA and ZEUS have been replaced with a full combined set with treatment of the correlated errors [7]. The HERA combined data on the $F_2^c(x, Q^2)$ structure function have been included [8]. Furthermore published HERA data for $F_L(x, Q^2)$ measurements have been included as well [9]. It has been decided to wait with the inclusion of Run II H1 and ZEUS until their combined data are available.

A whole range of Tevatron data sets have been included: CDF W–asymmetry data [10], D0 electron asymmetry data ($p_T > 25$GeV, 0.75fb^{-1}) [11] and D0 muon asymmetry data ($p_T > 25$GeV, 7.3fb$^-1$) [12]. In addition, the final numbers for CDF Z-rapidity data have been taken into account [13]. Overall, the inclusion of the mentioned sets do not have a major impact on the PDFs. The impact on α_S is rather moderate, too, with it changing to $\alpha_S = 0.1199$ from $\alpha_S = 0.1202$ at NLO, and changing to $\alpha_S = 0.1181$ from $\alpha_S = 0.1171$ at NNLO.
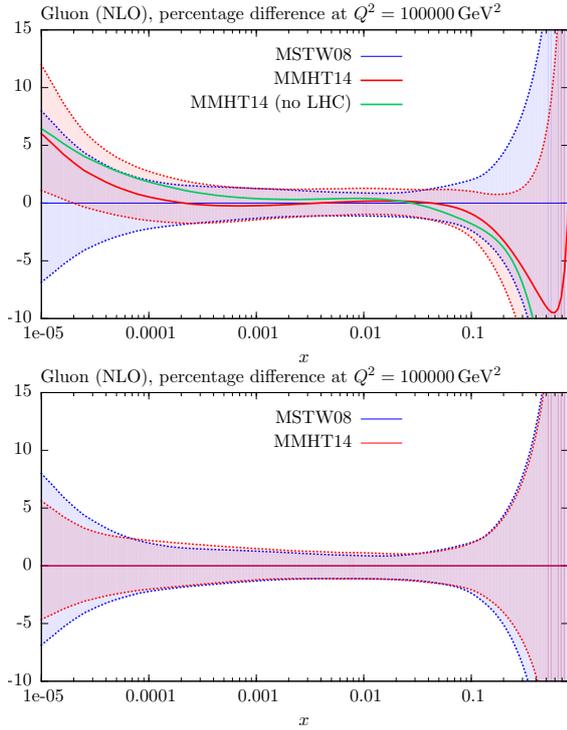
---

[1]Speaker.

Figure 1: Upper pane: the change in NLO gluon distribution when including LHC data. Lower pane: the change in uncertainty when including LHC data. The central value for MMHT without LHC is also shown.
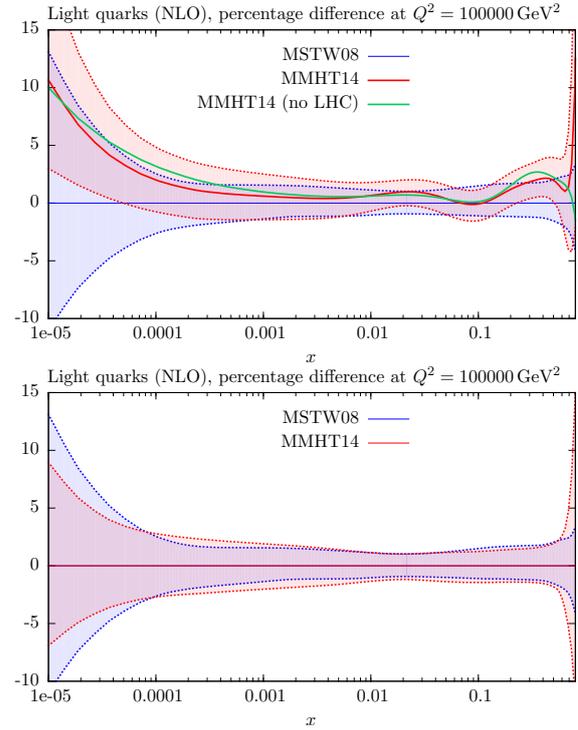

Figure 2: Upper pane: the change in NLO distribution of light flavour quarks when including LHC data. Lower pane: the change in uncertainty. The central value for MMHT without LHC is also shown.

2. Inclusion of LHC data

2.1. $W^\pm$, Z and $t\bar{t}$

The inclusion of LHC data has been vastly facilitated by software such as `FastNLO`, `APPLGrid`, `MCFM`, `DYNNLO` and `FEWZ`. For instance, ATLAS $W^\pm$ and Z–rapidity data can be included directly in the fit [14]. Before this inclusion the global fit yielded $\chi^2 \sim 1.6$ per point at NLO and $\chi^2 \sim 2$ per point at NNLO. After inclusion of the mentioned sets the value is brought down to $\chi^2 \sim 1.3$ at NLO, with the strongest pull being that on the gluon PDF. At NNLO the value is also brought down to $\chi^2 \sim 1.3$, with the largest impact being that on the strange distribution.

Whereas MSTW08 fits showed a poor behaviour for the u–quark valence distribution at low x, this is no longer an issue with the new parametrisation used, and the inclusion of LHC data leads to further improvements. Apart from including the ATLAS W, Z already mentioned, in MMHT, we also include CMS data on W–asymmetry (W's decaying into leptons) [15, 16], CMS Z–rapidity data [17], LHCb data

on $W^\pm$–production and $Z \to e^+e^-$ [18, 19], which all fit well at NLO. ATLAS high mass Drell-Yan data is also included and fits well, too.

More recently, we have also included the available data on $t\bar{t}$–production. More specifically this includes the combined cross section measurement from D0 and CDF as well as all published data from ATLAS and CMS at $\sqrt{S} = 7$TeV and one point at 8TeV. In doing so we have used $m_t = 172.5\pm1$ GeV. Both NLO and NNLO fits behave well, with the NLO fit preferring masses slightly below 172.5 GeV and NNLO slightly above.

2.2. Jet data

At NLO CMS jet data at $\sqrt{S} = 7$TeV [20] together with ATLAS $\sqrt{S} = 7$TeV [21] and $\sqrt{S} = 2.76$TeV data [22] have been included in the fit. The simultaneous fit with both the CMS and ATLAS jet data sets lead to visible improvements, with the biggest improvement being that for the CMS data.

The CMS experiment has released an update to the jet data [23]. Previously the single pion uncertainties were published correlated, but recently a decision within the
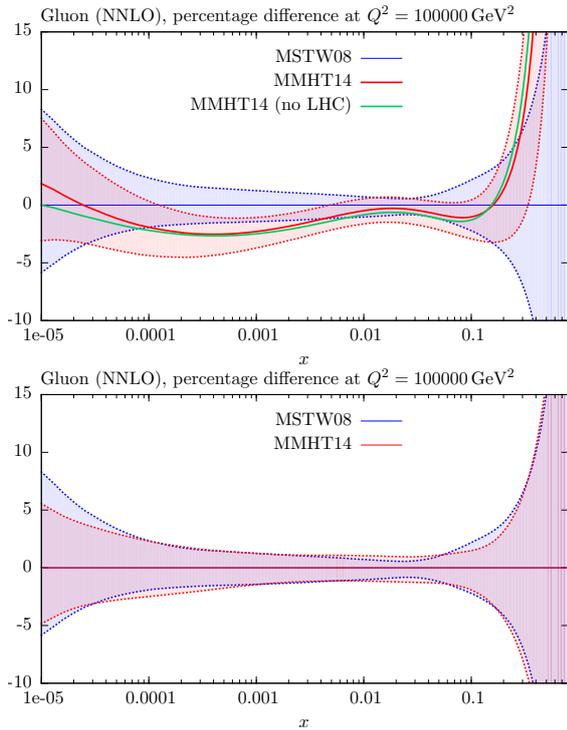
Figure 3: Upper pane: the change in NNLO gluon distribution when including LHC data. Lower pane: the change in uncertainty when including LHC data. The central value for MMHT without LHC is also shown.
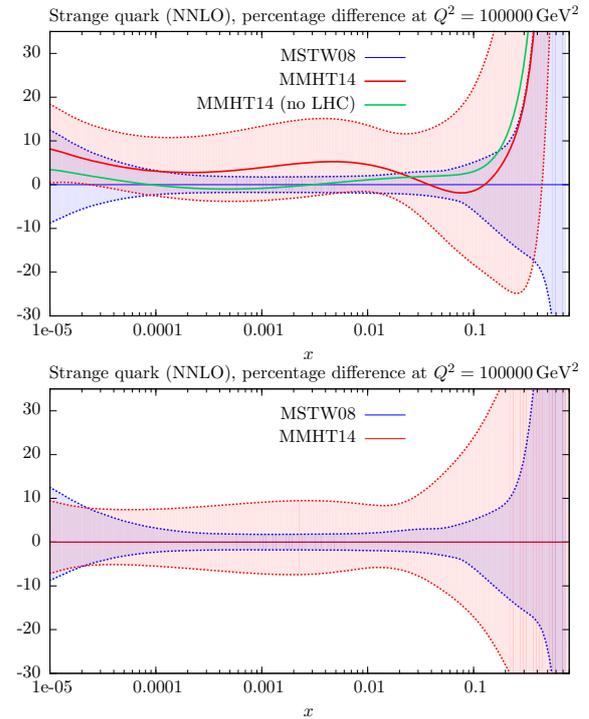

Figure 4: Upper pane: the change in NNLO gluon distribution when including LHC data. Lower pane: the change in uncertainty when including LHC data. The central value for MMHT without LHC is also shown.

collaboration was made to decorrelate the single pion systematics. In practice this means the single pion source of uncertainty has been split into five parts. We have taken the decorrelated systematics into account in our fits. This leads to an improvement for these data with χ^2 going from an initial 180 down to 140 and no major change in the PDFs.

2.2.1. Jet data at NNLO

When considering inclusive jet production at NNLO in the context of PDF fits the situation is far less unanimous than at NLO. While the usage of threshold corrections in the context of Tevatron jet data is well justified [24] as production there happens near threshold, in general, the situation is different for LHC data. Of course, for highish-x it is similar at both experiments but the frequency at which production happens near threshold is much lower than at the Tevatron. The threshold corrections tend to increase significantly as we move away from threshold and, as a consequence, the quality of the fit deteriorates [25].

The calculation of full fixed-order NNLO corrections for jet production are nearing completion [26, 27].

Preliminary results already give some indications of the full form of the corrections. Near threshold the agreement with previous existing corrections is good but as we move away from threshold we can expect (positive) large corrections. In [28] threshold corrections have been compared to full fixed order calculations for the gg–channel at NNLO for both the Tevatron and LHC. While the discrepancy between threshold and fixed order corrections remains below a certain level at the Tevatron, usually not more than 30-50% at high rapidity then at the LHC the discrepancy reaches levels of several hundred percent at high rapidity and low p_T. This strongly illustrates the need for full fixed order corrections in the theory description.

In MMHT we have investigated how sensitive the NNLO fits are to varying the K–factors. In order to do so, we applied very approximate NNLO corrections (ad hoc K–factor parametrisations) with positive corrections of ~5%-20%. The effects of applying a small and a large K–factor is show in Table 1. Neither of the K-factors change the PDFs much, with the smaller K–factor being the preferred. The changes are small

compared to the uncertainty, and although the fit is slightly worse than at NLO it remains comparable.

2.3. Doubly differential Drell-Yan at CMS

In the process of including LHC data into the PDF fits the doubly differential Drell-Yan data at CMS have been taken into account as well [29]. The comparison between data and theoretical predictions at both NLO and NNLO are shown in Fig. 2.4 for the two lowest mass bins. It seen that the NLO theory prediction describes the data rather poorly in the lowest mass bin, while NNLO is visibly closer to data. Things improve as we move higher up in mass. The LO component is very small in the lowest mass bin and what we see is the qualitative difference in description by the NLO and NNLO corrections in the low-mass limit.

2.4. Results

In Figs. 1 and 2 the impact of including LHC data on the gluon distribution and the light quark distributions, respectively, is shown at NLO. It is clear that the impact is limited in size with the most visible differences manifesting themselves at very low- and high x.

Figs. 3 and 4 show the impact of LHC data at NNLO on the gluon- and strange distributions, respectively. In the gluon case the change is rather moderate and, again, the uncertainty is lowered, generally. The strange distribution is seen to be affected significantly with the uncertainty becoming larger. This is predominantly due to the introduction of the charm to muon branching ratio of $B_\mu = 0.092$ with the sizeable accompanying uncertainty of $\pm 10\%$. At NNLO we extract the value $\alpha_S = 0.1172$. The overall effect of including LHC data has been summarised in Table 2. For NLO we see that the quality of the fit is improved by including LHC data and only in the case of the high-mass ATLAS Drell-Yan data are very slightly worse. In the NNLO case there is an overall improvement for all data, including the high-mass ATLAS Drell-Yan.

3. Conclusions

In the past years there has been ongoing work on updating the PDFs and an official PDF update is to be released very soon.

In the process we have seen the inclusion of the most up-to-date HERA and Tevatron data. Furthermore the most relevant published LHC data have been included as well: ATLAS, CMS and LHCb W, Z–data, $t\bar{t}$–cross
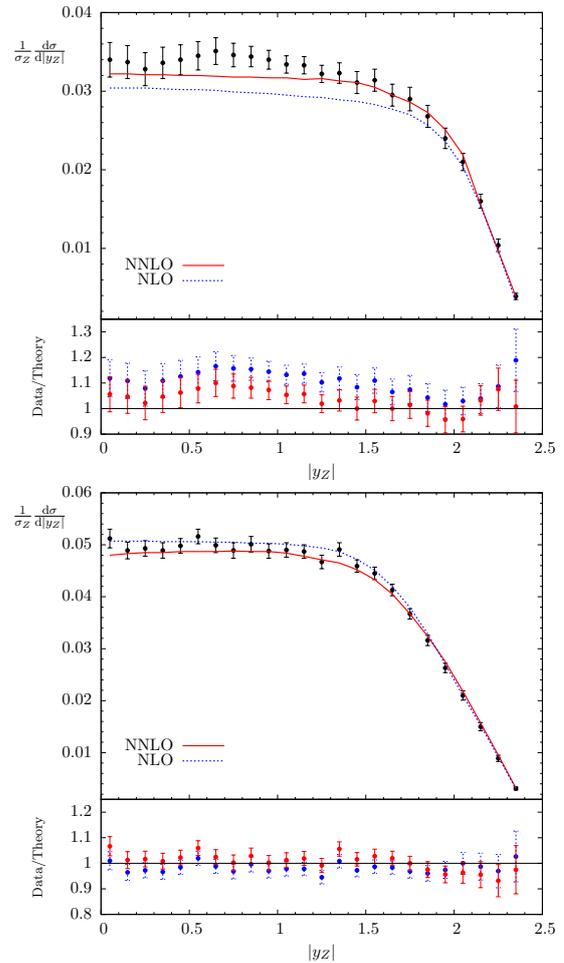

Figure 5: The two lowest mass bins for the doubly differential Drell-Yan cross section at CMS.

section data and all published ATLAS and CMS inclusive jet data, though the latter are currently not included at NNLO.

Inclusion of the mentioned data has so far had very few dramatic effects on the PDFs. The largest effect has been on the strange quark distribution (and mainly at NNLO) and low–x valence quarks, the latter largely due to change in methodology and newer data.

Currently there is some uncertainty in the manner the available NNLO corrections may affect the fits to jet data. Due to this it has been decided to wait with the inclusion of LHC jet data at NNLO until the full fixed order NNLO calculations are finalised.

data set	N_{pts}	MMSTWW Ref.[2]	MMHT2014 (no LHC)	MMHT2014 (with LHC)
NLO				
ATLAS jets (2.76 TeV+7 TeV)	116	107	107	106
CMS jets (7 TeV)	133	140	143	138
NNLO small K-factor				
ATLAS jets (2.76 TeV+7 TeV)	116	(107)	(123)	(119) 115
CMS jets (7 TeV)	133	(142)	(137)	(135) 137
NNLO large K-factor				
ATLAS jets (2.76 TeV+7 TeV)	116	(117)	(132)	(128) 126
CMS jets (7 TeV)	133	(145)	(137)	(139) 139

Table 1: The quality of the description (as measured by the value of χ^2) of the LHC inclusive jet data both before and after they have been included in the global NLO and NNLO fits. For comparison we also show the χ^2 values obtained in the CPdeut fit of the NLO MMSTWW analysis [2], which did not include LHC data. The bracketed numbers are for the cases where the LHC jet data was not included in the NNLO fit.

References

[1] A. D. Martin, W. J. Stirling, R. S. Thorne, G. Watt, Parton distributions for the LHC, Eur.Phys.J. C63 (2009) 189–285. arXiv:0901.0002, doi:10.1140/epjc/s10052-009-1072-5.

[2] A. D. Martin, A. J. T. Mathijssen, W. J. Stirling, R. S. Thorne, B. J. A. Watt, et al., Extended Parameterisations for MSTW PDFs and their effect on Lepton Charge Asymmetry from W Decays, Eur.Phys.J. C73 (2013) 2318. arXiv:1211.1215, doi:10.1140/epjc/s10052-013-2318-9.

[3] R. S. Thorne, Effect of changes of variable flavor number scheme on parton distribution functions and predicted cross sections, Phys.Rev. D86 (2012) 074017. arXiv:1201.6180, doi:10.1103/PhysRevD.86.074017.

[4] M. Goncharov, et al., Precise measurement of dimuon production cross-sections in muon neutrino Fe and muon anti-neutrino Fe deep inelastic scattering at the Tevatron, Phys.Rev. D64 (2001) 112006. arXiv:hep-ex/0102049, doi:10.1103/PhysRevD.64.112006.

[5] T. Bolton, Determining the CKM parameter V(cd) from neutrino N charm productionarXiv:hep-ex/9708014.

[6] G. D'Agostini, On the use of the covariance matrix to fit correlated data, Nucl.Instrum.Meth. A346 (1994) 306–311. doi:10.1016/0168-9002(94)90719-6.

[7] F. Aaron, et al., Combined Measurement and QCD Analysis of the Inclusive e+- p Scattering Cross Sections at HERA, JHEP 1001 (2010) 109. arXiv:0911.0884, doi:10.1007/JHEP01(2010)109.

[8] H. Abramowicz, et al., Combination and QCD Analysis of Charm Production Cross Section Measurements in Deep-Inelastic ep Scattering at HERA, Eur.Phys.J. C73 (2013) 2311. arXiv:1211.1182, doi:10.1140/epjc/s10052-013-2311-3.

[9] S. Chekanov, et al., Measurement of the Longitudinal Proton Structure Function at HERA, Phys.Lett. B682 (2009) 8–22. arXiv:0904.1092, doi:10.1016/j.physletb.2009.10.050.

[10] T. Aaltonen, et al., Direct Measurement of the W Production Charge Asymmetry in $p\bar{p}$ Collisions at $\sqrt{s}$ = 1.96 TeV, Phys.Rev.Lett. 102 (2009) 181801. arXiv:0901.2169, doi:10.1103/PhysRevLett.102.181801.

[11] V. Abazov, et al., Measurement of the electron charge asymmetry in $p\bar{p}$ → W + X → ev + X events at $\sqrt{s}$ = 1.96-TeV, Phys.Rev.Lett. 101 (2008) 211801. arXiv:0807.3367, doi:10.1103/PhysRevLett.101.211801.

[12] V. M. Abazov, et al., Measurement of the muon charge asymmetry in $p\bar{p}$ → W+X → $\mu\nu$ + X events at $\sqrt{s}$=1.96TeV, Phys.Rev. D88 (2013) 091102. arXiv:1309.2591, doi:10.1103/PhysRevD.88.091102.

[13] T. A. Aaltonen, et al., Measurement of $d\sigma/dy$ of Drell-Yan e^+e^- pairs in the Z Mass Region from $p\bar{p}$ Collisions at $\sqrt{s}$ = 1.96 TeV, Phys.Lett. B692 (2010) 232–239. arXiv:0908.3914, doi:10.1016/j.physletb.2010.06.043.

[14] G. Aad, et al., Measurement of the inclusive $W^\pm$ and Z/gamma cross sections in the electron and muon decay channels in pp collisions at $\sqrt{s}$ = 7 TeV with the ATLAS detector, Phys.Rev. D85 (2012) 072004. arXiv:1109.5141, doi:10.1103/PhysRevD.85.072004.

[15] S. Chatrchyan, et al., Measurement of the lepton charge asymmetry in inclusive W production in pp collisions at $\sqrt{s}$ = 7 TeV, JHEP 1104 (2011) 050. arXiv:1103.3470, doi:10.1007/JHEP04(2011)050.

[16] S. Chatrchyan, et al., Measurement of the electron charge asymmetry in inclusive W production in pp collisions at $\sqrt{s}$ = 7 TeV, Phys.Rev.Lett. 109 (2012) 111806. arXiv:1206.2598, doi:10.1103/PhysRevLett.109.111806.

[17] S. Chatrchyan, et al., Measurement of the Rapidity and Transverse Momentum Distributions of Z Bosons in pp Collisions at $\sqrt{s}$ = 7 TeV, Phys.Rev. D85 (2012) 032002. arXiv:1110.4973, doi:10.1103/PhysRevD.85.032002.

[18] R. Aaij, et al., Inclusive W and Z production in the forward region at $\sqrt{s}$ = 7 TeV, JHEP 1206 (2012) 058. arXiv:1204.1620, doi:10.1007/JHEP06(2012)058.

[19] R. Aaij, et al., Measurement of the cross-section for $Z \to e^+e^-$ production in pp collisions at $\sqrt{s}$ = 7 TeV, JHEP 1302 (2013) 106. arXiv:1212.4620, doi:10.1007/JHEP02(2013)106.

[20] S. Chatrchyan, et al., Measurements of differential jet cross sec-

data set	N_{pts}	MMSTWW Ref.[2]	MMHT2014 (no LHC)	MMHT2014 (with LHC)
NLO				
ATLAS W^+, W^-, Z	30	47	44	38
CMS W asymm $p_T > 35$ GeV	11	9	16	7
CMS asymm $p_T > 25$ GeV,30 GeV	24	9	17	8
LHCb $Z \to e^+e^-$	9	13	13	13
LHCb W asymm $p_T > 20$ GeV	10	12	14	12
CMS $Z \to e^+e^-$	35	21	22	19
ATLAS high-mass Drell-Yan	13	20	20	21
CMS double diff. Drell-Yan	132	385	396	373
NNLO				
ATLAS W^+, W^-, Z	30	72	53	39
CMS W asymm $p_T > 35$ GeV	11	18	15	8
CMS asymm $p_T > 25$, 30 GeV	24	18	17	9
LHCb $Z \to e^+e^-$	9	23	22	21
LHCb W asymm $p_T > 20$ GeV	10	24	21	18
CMS $Z \to e^+e^-$	35	30	24	22
ATLAS high-mass Drell-Yan	13	18	16	17
CMS double diff. Drell Yan	132	159	151	149

Table 2: The quality of the description (in terms of χ^2) of the LHC W, Z data before and after they are included in the global NLO and NNLO fits. χ^2 values obtained in the CPdeut fit of the NLO MMSTWW analysis [2] are shown for comparison. The data included were identical to those in MSTW08.

tions in proton-proton collisions at $\sqrt{s}$ = 7 TeV with the CMS detector, Phys.Rev. D87 (11) (2013) 112002. arXiv:1212.6660, doi:10.1103/PhysRevD.87.112002.

[21] G. Aad, et al., Measurement of inclusive jet and dijet production in pp collisions at $\sqrt{s}$ = 7 TeV using the ATLAS detector, Phys.Rev. D86 (2012) 014022. arXiv:1112.6297, doi:10.1103/PhysRevD.86.014022.

[22] G. Aad, et al., Measurement of the inclusive jet cross section in pp collisions at sqrt(s)=2.76 TeV and comparison to the inclusive jet cross section at sqrt(s)=7 TeV using the AT-LAS detector, Eur.Phys.J. C73 (2013) 2509. arXiv:1304.4739, doi:10.1140/epjc/s10052-013-2509-4.

[23] C. Collaboration, PDF constraints and extraction of the strong coupling constant from the inclusive jet cross section at 7 TeV.

[24] N. Kidonakis, J. Owens, Effects of higher order threshold corrections in high E(T) jet production, Phys.Rev. D63 (2001) 054019. arXiv:hep-ph/0007268, doi:10.1103/PhysRevD.63.054019.

[25] B. Watt, P. Motylinski, R. Thorne, The Effect of LHC Jet Data on MSTW PDFs, Eur.Phys.J. C74 (2014) 2934. arXiv:1311.5703, doi:10.1140/epjc/s10052-014-2934-z.

[26] A. Gehrmann-De Ridder, T. Gehrmann, E. Glover, J. Pires, Second order QCD corrections to jet production at hadron colliders: the all-gluon contribution, Phys.Rev.Lett. 110 (16) (2013) 162003. arXiv:1301.7310, doi:10.1103/PhysRevLett.110.162003.

[27] J. Currie, A. Gehrmann-De Ridder, E. Glover, J. Pires, NNLO QCD corrections to jet production at hadron colliders from gluon scattering, JHEP 1401 (2014) 110. arXiv:1310.3993, doi:10.1007/JHEP01(2014)110.

[28] S. Carrazza, J. Pires, Perturbative QCD description of jet data from LHC Run-I and Tevatron Run-IIarXiv:1407.7031.

[29] S. Chatrchyan, et al., Measurement of the differential and double-differential Drell-Yan cross sections in proton-proton collisions at $\sqrt{s}$ = 7 TeV, JHEP 1312 (2013) 030. arXiv:1310.7291, doi:10.1007/JHEP12(2013)030.